tvst

DOI: 10.1167/tvst.5.4.16

Article

Retinal Arterioles in Hypo-, Normo-, and Hypertensive Subjects Measured Using Adaptive Optics

Jacob G. Hillard, Thomas J. Gast, Toco Y.P. Chui, Dan Sapir, and Stephen A. Burns

Indiana University, Bloomington, IN, USA

Correspondence: Stephen A. Burns, 800 E. Atwater, Indiana University, Bloomington, IN, USA. e-mail: staburns@indiana.edu

Received: 9 March 2016
Accepted: 7 July 2016
Published: 31 August 2016

Keywords: retinal vessels; vascular diseases; hemodynamics; arterioles; optical imaging; adaptive optics

Citation: Hillard JG, Gast TJ, Chui TYP, Sapir D, Burns SA. Retinal arterioles in hypo-, normo-, and hypertensive subjects measured using adaptive optics. Trans Vis Sci Tech. 2016;5(4):16, doi:10.1167/tvst.5.4.16

Purpose: Small artery and arteriolar walls thicken due to elevated blood pressure. Vascular wall thickness show a correlation with hypertensive subject history and risk for stroke and cardiovascular events.

Methods: The inner and outer diameter of retinal arterioles from less than 10 to over 150 μm were measured using a multiply scattered light adaptive optics scanning laser ophthalmoscope (AOSLO). These measurements were made on three populations, one with habitual blood pressures less than 100/70 mm Hg, one with normal blood pressures without medication, and one with managed essential hypertension.

Results: The wall to lumen ratio was largest for the smallest arterioles for all three populations. Data from the hypotensive group had a linear relationship between outer and inner diameters ($r^2 = 0.99$) suggesting a similar wall structure in individuals prior to elevated blood pressures. Hypertensive subjects fell below the 95% confidence limits for the hypotensive relationship and had larger wall to lumen ratios and the normotensive group results fell between the other two groups.

Conclusion: High-resolution retinal imaging of subjects with essential hypertension showed a significant decrease in vessel inner diameter for a given outer diameter, and increases in wall to lumen ratio and wall cross-sectional areas over the entire range of vessel diameters and suggests that correcting for vessel size may improve the ability to identify significant vascular changes.

Translational Relevance: High-resolution imaging allows precise measurement of vasculature and by comparing results across risk populations may allow improved identification of individuals undergoing hypertensive arterial wall remodeling.

Introduction

The human eye offers direct optical access to the retina, a portion of the central nervous system, and its vasculature, using noninvasive optical techniques. Because of this accessibility changes in the retinal vessels have long been considered as potential biomarkers for systemic vascular diseases[1–4] and improved clinical instruments[5–9] have enhanced our ability to measure properties of the retinal vascular bed. In the past, these measurements were limited to the larger retinal vessels unless exogenous contrast agents such as fluorescein were used. Nonetheless, systemic diseases such as hypertension and diabetes have well documented relationships with retinal vessel structure and regulatory responses.[2,10,11] In recent years, the development of adaptive optics (AO) retinal imaging,[12–22] and optical coherence tomography (OCT)[23,24] have provided clinicians and scientists with improved information on retinal vascular changes. With the recent advances in imaging of the vasculature[25–30] we now have tools available to provide precise structural measurements of retinal vessels from the largest retinal vessels down to the capillaries. It has recently been demonstrated that AO retinal imaging can show hypertensive changes in the walls of retinal vessels with great precision.[22]

The current work uses AO-assisted retinal imaging to measure the impact of essential hypertension (HTN) on the walls of the retinal arteries and arterioles. It is thought that in essential HTN, changes in blood vessel structure leads to increased resistance to blood flow.[31,32] This increase in resistance is thought to occur first at a level of the vasculature known as "resistance vessels" that, by definition, control the blood pressure of the system. Although

the actual size of these resistance vessels is not well known, they are usually thought to be smaller than 350 μm in outer diameter (OD).[33] With the advent of HTN there are changes in vascular walls, but these are initially reversible. However, once the pressure of the system has been elevated for a sufficient duration, a positive-feedback cycle effects the vascular wall structure.[32,34] For vessels larger than about 300 μm in diameter the increase in vessel wall thickness occurs without changing the lumen diameter, or inner diameter (ID), a process known as outward hypertrophic remodeling.[34] In small arteries remodeling is thought to occur differently. The total volume of the vascular wall remains constant but both the OD and the ID each decrease,[35] a process known as inward eutrophic remodeling.[34,36,37] These processes may not be independent, subcutaneous and retinal arteries may use a combination of eutrophic and hypertrophic remodeling dependent on the degree and duration of hypertension, but the retinal response being primarily eutrophic.[35,38,39] The hypertrophic form of vascular remodeling seems to be particularly associated with an elevated risk of cerebrovascular and cardiovascular risk[40,41] and any improvement in noninvasive detection and classification of vascular remodeling would be valuable.

In general, changes to the vascular walls are typically quantified using a ratio measure comparing the wall thickness with the lumen diameter, the wall to lumen ratio (WLR). WLR is correlated to HTN[37,38,42] and can be measured in relatively large vessels of the eye using a scanning laser Doppler flowmeter.[42–44] Recently Koch et al.[22] used a commercially available flood illuminated AO retinal camera to show increased WLR in HTN, and together with other studies, the results suggest that smaller vessels are better indicators of hypertensive changes in the eye.[22,43]

The purpose of this study was to use an AO scanning laser ophthalmoscope (AOSLO) with multiply scattered light detection providing higher contrast of vessel wall structure,[27,29,45] to measure WLRs over the full range of retinal vessels and in particular to test whether arterioles smaller than 50 μm in ID have a larger difference between the WLR of hypertensive subjects and normotensive (NTN) subjects. In an attempt to better refine the relationship between blood pressure and vascular wall anatomy, we included a third group of otherwise healthy subjects with a life-long history of nonpathological low blood pressures.

Methods

Subjects

Fifty-five subjects were recruited for study by use of poster advertisements and referral from local physicians. Subjects were classified as HTN if they had been physician diagnosed as such, and were on any type of antihypertensive medication. Subjects were classified as NTN if they had never been diagnosed as hypertensive and never taken antihypertensive medications. Subjects were place into a third group, which we called hypotensive (LTN) if they met the classification of NTN, but also self-reported that their blood pressure had rarely been above 100/70 mm Hg and were fully functional without a medical condition producing hypotension. For subanalyses, we divided subjects into two age groups, a younger (<40 years) group and an older group (≥40 years). All subjects were examined by an ophthalmologist. No subjects had signs of retinal hypertensive pathology other than a few subjects with arteriovenous nicking or vascular tortuosity. Careful medical histories were taken with a focus on causes of secondary hypertension, subjects were excluded from the study if they had any relevant systemic diseases other than essential HTN. Subject characteristics and statistics by group are given in Table 1. The population was primarily Caucasian, with four Asians and no African Americans. All subjects were informed of the risks and benefit of participating in the study and all procedures in this study were approved by the institutional review board of Indiana University and adhered to the tenets of the Declaration of Helsinki.

Imaging

We used the Indiana AOSLO.[46] This produces near-diffraction limited performance when imaging the retina in vivo.[47] The system can work with pupil sizes up to 8 mm,[48] although as expected the pupil size is inversely related to the resolution. For an 8-mm pupil, the lateral resolution using 820-nm light is approximately 2 μm. Axial resolution is dependent on the size of the confocal aperture and the spatial frequency of the target. In general, Axial focusing within 20 μm was required for optimal vessel wall images. The system incorporates a steering system that allows us to relate the small-field AOSLO image to locations on a previously obtained wide field fundus image from a commercial retinal imaging

Table 1. Subject Characteristics

Statistics	HTN (%)	NTN (%)	LTN (%)
All data	23	22	10
Number of males	15 (65%)	14 (64%)	1 (10%)
Number of females	8 (35%)	8 (36%)	9 (90%)
Over 40	20 (86%)	10 (45%)	3 (30%)
Under 40	3 (13%)	12 (55%)	7 (70%)
Average age	52.9	37.5	33.2
Average age (older group)	57.6	53.8	52.66
Average age (younger group)	22	23.9	24.8
SD age	13.73	15.59	13.73

system (Heidelberg Spectralis, Heidelberg, Germany).[49] The AOSLO system also allows us to fully control our confocal aperture at the detector plane, choosing one of several aperture diameters, as well as changing its location in 2 dimensions.[50]

Procedure

All subjects had an ophthalmic exam including visual acuities, a slit-lamp examination, and a dilated fundus examination. If the dilated exam did not take place immediately before the AOSLO imaging, one drop of tropicamide 0.5% ophthalmic solution was distilled into the study eye. Axial length (AL) measurements were taken with a Zeiss IOL Master Version 5 (Carl Zeiss Meditec, Dublin, CA) for retinal image magnification calculations. Fundus images and OCT scans were then obtained on all subjects using a Heidelberg Spectralis system. If image quality of the OCT scans was not high, or was variable, artificial tears were given to the subject.

Experimental Imaging

The AOSLO imaging beam was 820 nm (12 nm half-width) and the wavefront sensing was at 870 nm (powers measured at the cornea were 100 and 50 μW, respectively). All light levels used were safe according to ANSI standards for safe use of laser light.[51] A single eye was measured for each subject. AOSLO images were obtained by sequentially imaging along a retinal artery, starting with arteries approximately 1500 μm from the center of the optic disc and following along successive branches until the walls of the arteriole were too small to resolve. For most subjects all AOSLO experimental images were obtained in a single session with frequent short breaks. A data collection session took approximately 40 minutes.

To enhance the visibility of vessel walls a relatively large confocal aperture (10× the Airy disc diameter), displaced by more than the aperture radius was used.[26] For the best quality image, the confocal aperture was offset along the direction of blood flow in the vessel, which was known from the anatomy of the retinal quadrant being imaged. Image focus was adjusted as needed to keep the vessel walls in focus, and the scan size of the system was adjusted from 1.7° to approximately 1.14° for the smallest vessels (at a pixel size of 520 × 570 pixels after correction for scan distortion). Field sizes were automatically recorded by the imaging system.

To obtain an image of a vessel the operator first optimized the focus of the image watching a live view of the retina. When a good image was achieved, the operator signaled the computer by a mouse click or foot switch and approximately 100 sequential frames of video were recorded at a rate of 28 frames per second.

Image Processing/Measurements

Image processing was performed semiautomatically offline after the completion of the data collection as has been described elsewhere.[29] Briefly, images were first corrected for the sinusoidal distortion produced by the scanning method and individual video frames were then eliminated if blinks, poor image quality, or large eye movement within a frame was detected. The remaining frames of the video were then aligned to a template frame automatically chosen by the software based on minimal eye motion between two successive frames. Small eye movements both between and within each frame were corrected as successive frames were aligned to the template frame. The final output consisted of a short video clip for each region of the blood vessel, an average image,[52] and a SD image[25] that provided a map of the vascular perfusion. The

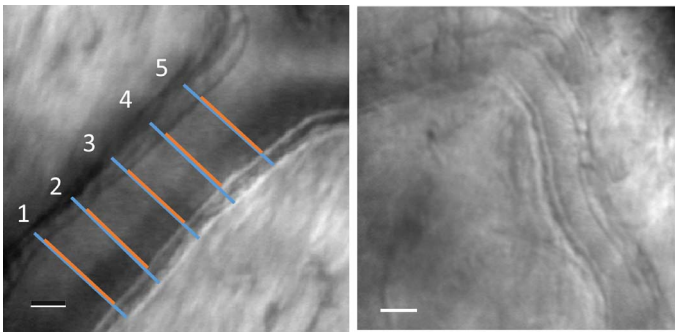

Figure 1. *Left*: A retinal arteriole imaged with multiply scattered light in the AOSLO. The OD was defined as the distance between the outer edges of the vessel walls and was measured five times, spaced at roughly the lumen diameter (*blue lines*). The ID was defined as the lumen diameter, and the lumen was confirmed by examining video segments for visualized blood flow as well as perfusion maps of the vessel. The ID was similarly measured five times (*red lines*). *Red and blue lines* have been displaced slightly for clarity. *Right*: A smaller arteriole from a different normal subject. The *scale bars* represent 25 μm.

averaging of the image improved grading of the vessel by reducing noise and the SD image showed the areas of erythrocyte movement, aiding in identification of vessel lumens.

Quantification of lumens and walls was performed manually in Photoshop (Adobe Systems, Inc., San Jose, CA) by masked graders. We first selected arterioles by comparing the small field AOSLO images to the 30° clinical SLO fundus images, ensuring we followed an arteriole during image acquisition. It was also possible to distinguish the direction of red blood cell motion based on the video segments. From these arterioles we then selected images that contained areas of measureable contrast between the vessel wall and both the retina and the vessel lumen. The grader made measurements in a location where the vessel was approximately straight for a length of at least 10 times the ID of the vessel and the vessel was without bifurcation. All measurements were taken in a direction perpendicular to the vessel wall.

The distance from the outside of the vessel wall to the outside of the contralateral vessel wall was called the OD of the vessel (Fig. 1). This measurement was recorded, and then at the same location the distance from just inside the vessel wall to just inside the contralateral vessel wall was recorded as the ID. Both the OD and the ID for each vessel image were measured five times with the location of each individual pair of OD and ID measurements displaced from the previous measurement by approximately the ID of the vessel.

Table 2. Definitions of Computations Used in the Current Paper

(1)	$RM = ((AL - 24) + 16.53) / (16.53)$
(2)	$WT = (OD\text{-}ID)/2$
(3)	$WLR = (OD\text{-}ID)/ID$
(4)	$WT_1 = (ID+1\ wall)\text{-}\ ID)$
(5)	$WLR_1 = (WT_1 * 2) / (ID)$
(6)	$WCSA = (\pi (OD^2 - ID^2)) / (4)$

RM = retinal magnification, AL = axial length, WT = wall thickness, OD = outer diameter, IU = inner diameter, WLR = Wall to Lumen Ratio, WCSA = Wall Cross-Sectional Area; subscript of 1 indicates computation when only one wall was clearly visualized.

Magnification was taken into account when analyzing the data by use of a simple formula (Table 2) and the axial length measurements. Magnification differences between scan sizes are a known property of the system and were also taken into account.

Some vessel images could not be measured due to shadowing, or because the focus was in a different plane than the vessel. Images where the contrast of the vessel wall was deemed uncertain by the grader were not measured and therefore, not used in any calculations. The WLR was calculated as the difference between the OD and ID divided by the ID. In a some cases (20 of 370), shadowing on one side of the vessel prevented precise localization of one of the outer walls of the vessel, and in this case a measurement from the outside of the vessel wall on the side with good contrast to the inside of the contralateral vessel wall was taken. In these cases the WLR was calculated assuming radial symmetry of the vessel. In all cases, when measuring the vessel lumen, it was differentiated from the vessel wall by visible structural differences and was verified when needed by movement of erythrocytes seen in aligned video sequences.

Variability of Measurements

Interobserver variability of the manual grading of WLR was measured by having a second expert grader blindly regrade both the ID and OD of 21 vessel locations from 18 subjects. The measurements were then compared with the original grader's results. On average, the two graders agreed within 2% on vessel size and the interclass correlation for this comparison was 0.99. For this reason, only the original grader's measurements were used for analysis.

Calculations

Calculations were made based on the equations in Table 2. The retinal magnification (RM) due to ocular AL for each subject was calculated using Equation 1[53] and the subject's AL obtained from the Zeiss IOL Master. This calculation became necessary to compare the absolute vessel sizes across subjects. Wall thickness (WT) was calculated using Equation 2. WLR was calculated using Equation 3.

In 5.4% of images in which the OD was measured using the one sided method, wall thickness was calculated using Equation 4. For these images the WLR was calculated using Equation 5. Wall cross-sectional area (WCSA) calculations are shown in Equation 6.

Statistical Analysis

We analyzed data in two ways. Primary statistical analyses were performed by first pooling multiple measures within a vessel size category for each subject. Pooling was performed to compare subject groups for WCSA and WLR, which had a strong dependence on vessel size. Thus, it was necessary to avoid weighing each subject differently based on the number and location of measured blood vessels. For each subject we included all measured vessel locations (an average of 7 locations per subject), and grouped vessels into three size classes, indicating whether their ID was less than 10 μm (Class 1), between 10 and 50 μm (Class 2), and larger than 50 μm (Class 3). We then calculated the average WLR data from each subject for each vessel class. For the analysis of the variance (ANOVA), we included only vessels in classes 2 and 3. The primary analysis was a two-way ANOVA of WLR, vessel size, and blood pressure status. Post hoc comparisons of WLR as a function of vessel size class were made within each blood pressure group and for a given size across blood pressure groups using Student's *t*-test. We also performed regression analysis to determine the relation of ID and OD for the different subject groups.

Results

Measurability

In general, we were able to make measurements in almost all subjects for all locations selected for imaging. Across all subjects we could not quantify vessel properties for 14 of 370 imaged artery locations (3.8%) due to shadowing or nonoptimal plane of focus. Twenty arterioles were graded using the "one sided method" out of the total 370 artery locations picked for measurement (5.4%).

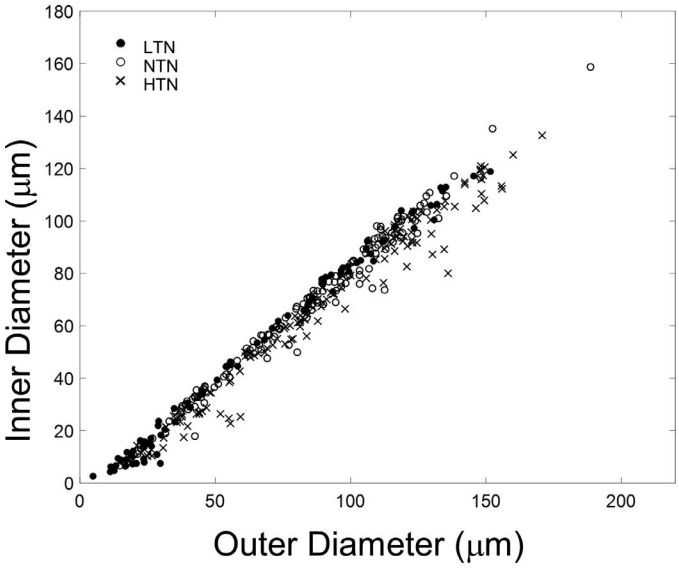

Figure 2. Vessel ID plotted as a function of OD for all measured vessels in LTN (*filled circles*), NTN (*open circles*), and HTN (*crosses*) subjects.

Vascular Structural Measurements

Vascular ID varied with both vessel size and blood pressure status. Figure 1 shows example results from normal subjects for two sizes of vessels. Here, we see that the vascular wall was clearly imaged and measurable. Vessel ID ranged in size from 3 to 169 μm and OD ranged from 6 to 216 μm (Fig. 2). ID and OD were highly correlated for all three subject groups (r^2 of 0.993, 0.982, and 0.973 for LTN, NTN, and HTN groups, respectively, Fig. 3).

Wall to Lumen Ratio

WLR varied with vessel diameter (Fig. 4). The largest WLR occurred in the smallest vessels that were measureable, which were vessels under 10 μm in lumen diameter. While some vessels with ID of less than 10 μm were measurable in all subject groups, 17 of the 22 (77.27%) vessels in this size range were measured in the LTN group, perhaps partially due to their younger age (Table 1) providing higher contrast images. Therefore, we excluded from our statistical analysis vessels smaller than 10 μm in ID (class 1 vessels). For vessels above 10 μm in ID the largest WLR occurred among the smallest measurable vessels of the HTN subjects (Fig. 4) with 9 of 10 of the largest WLR measurements occurring in HTN subjects. The

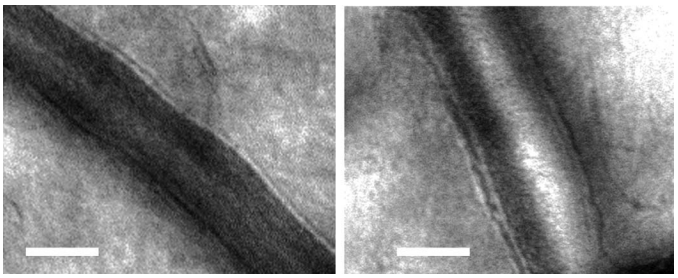

Figure 3. Retinal arteriole from a LTN subject (*left*) with a WLR of 0.22, compared with a similar sized vessel from a hypertensive subject (*right*) with a WLR of 0.34. The *scale bar* represents 50 μm. Contrast of images was stretched for display purposes.

WLR's for our class 2 vessels were 0.44 ± 0.20, 0.41 ± 0.23, and 0.70 ± 0.38 for the LTN, NTN, and HTN subjects, respectively (Fig. 5). WLR was smaller for the class 3 vessels, with WLR's of 0.211 ± 0.196, 0.234 ± 0.078, and 0.303 ± 0.084 for LTN, NTN, and HTN subjects, respectively. The two-way ANOVA for WLR, calculated using averages for each subject for each size category, revealed a significant relation between both WLR and vessel size and WLR and HTN status, with WLR depending on vessel size class ($P < 0.0001$) and blood pressure group ($P < 0.0001$). Vessel size and blood pressure status interacted significantly ($P = 0.0385$). These interactions all persisted when comparing only the NTN and HTN groups. The WLR of the NTN and LTN groups were not significantly different from each other ($P > 0.7$), although in general data from the LTN group showed a more systematic relation between OD and WLR and other measures (see below). We examined the data for significance of age and also of sex and no significant differences within groups were seen.

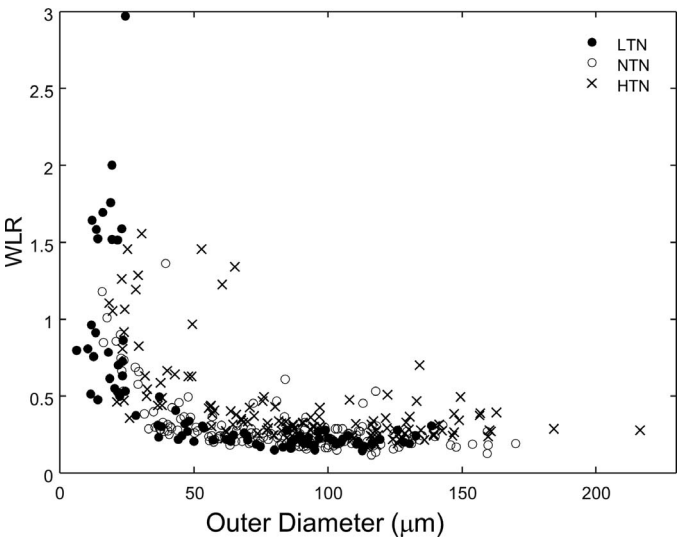

Figure 4. The dependence of the WLR on the OD. While we measured vessels with an ID less than 10 μm, these were primarily measurable in our LTN subjects (*filled symbols*), and therefore were not included in the statistical analyses.

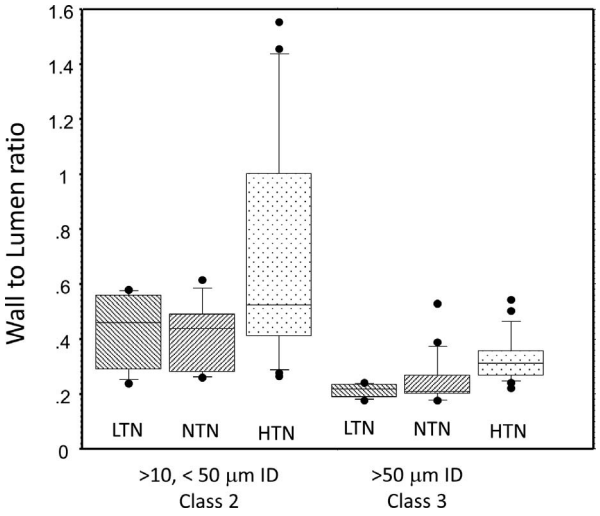

Figure 5. Comparison of WLR for different subject groups. Vessels smaller than 10 μm were excluded from this analysis and the data for each subject within a size class were averaged and then analyzed. The median for each group is shown as the *center horizontal line*, the *box* encloses the 25th to 75th percentiles and the *whiskers* are set to enclose 80% of the data; *symbols* represent subjects with either a WLR in the top 10% or bottom 10% of the sample.

Wall Cross-Sectional Area

WCSA increased with vessel size (Fig. 6). HTN subjects had larger WCSA than NTN subjects for both size classes of vessels ($P = 0.025$ and $P = 0.01$, unpaired t-test for small and large size classes, respectively). For the comparison of HTN and LTN subjects the difference for small vessels was not significant ($P = 0.06$) but was for the larger vessels ($P = 0.008$).

Discussion

The finding of increased WLR in HTN agrees with previous studies,[22,38,54,55] now using multiply scattered light AOSLO imaging. Our results are similar to the increased WLR with HTN reported by Koch et al.[22] with a flood illuminated AO camera, but we cover an even larger range of sizes. The hypertensive subjects in this study were treated, whereas those in Koch were untreated. To allow us to compare our results more directly with Koch et al.,[22] as well as to studies that used scanning laser Doppler flowmetry

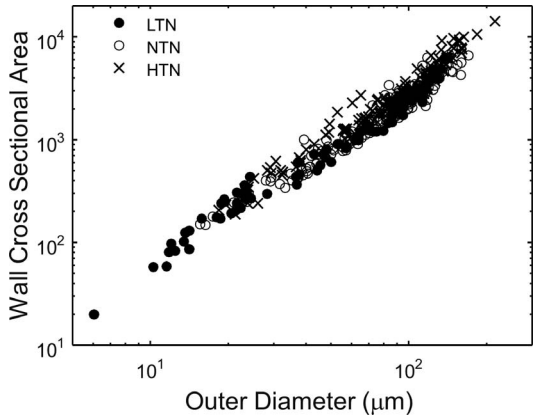

Figure 6. Vessel WCSA and OD are compared on log axes.

on slightly larger vessels,[35,40,54,55] we formed a subset of our data including all vessels between 90 and 120 μm ID. Our data, while having slightly thinner walls for a given lumen, show similar WLR and impact of hypertension, whether treated or not (Table 3). All techniques show thickened walls in the hypertensive groups although not significantly for the Baleanu[35] study. While our WLR measurements were smaller than the others, as seen in Figures 1 and 3, the walls were well delineated and measurements were replicable. The results from all these retinal studies are consistent with HTN producing increased WLR in the central nervous system.[40]

We examined the relation of ID to OD, which is important both for understanding how vessels remodel[56] and for determining whether there is a fundamental relation between wall thickness and lumen diameter. The data of Figure 2, demonstrate that both the LTN and NTN subjects' vessels have a very tight linear relationships between ID and OD. In particular, there seems to be an upper bound to the ID for each OD formed by the data from the LTN subjects. Data from the NTN and HTN subjects fall on or below this line. This suggests a deterministic relationship between vessel diameter and the wall thickness prior to vascular remodeling. Linear correlation between the outer and inner vascular diameters for the LTN group had an r^2 greater than 0.99 (Fig. 2) and the NTN data were close but fall slightly below the LTN group and the HTN data fall even further below, with the HTN group outside the 95% confidence limits of both the LTN and NTN groups. This paints a consistent picture of the LTN data representing a "basal" state for the vasculature and NTN and hypertensive data resulting from eutrophic remodeling.

The assumption, that the line formed by the LTN data represents an estimate of the initial state from which vessels are eutrophically remodeled, allows us to model the impact of vascular remodeling as depicted in Figure 7. Here the solid diagonal line with a slope of 0.88 is the linear fit to the LTN data of Figure 6. Eutrophic remodeling conserves WCSA for a given vessel ID and OD. This causes a vessel to move down and to the left, as illustrated by the dashed curved lines, because as the outer wall moves inward, the ID shrinks even more. Remodeled vessels lie somewhere within the space below and to the right of the baseline. We can relate each current hypertensive data point to a position on the LTN line, which has the same WCSA (the curved line with an arrow shows possible WCSA conserving positions from an initial starting data point). Using the empirically defined relations we can ask (1) are they consistent with eutrophic remodeling that is expected for vessels of this size in HTN, and (2) what is the impact of remodeling on vascular resistance? In Figure 7 we see that all data fall within the range of values consistent with eutrophic remodeling. However, our results could be consistent with other types of remodeling. To determine whether the data suggest hypertrophic remodeling we fit WCSA versus OD for all vessels with a three parameter power model and computed 95% confidence intervals (CIs). While there was a trend for the large vessels to have larger WCSA, the

Table 3. Comparison of WLR between Normal and Treated Hypertensive Subjects across Studies

	WLR NTN	WLR HTN	Significance
Current paper	0.210 ± 0.05	0.280 ± 0.08	Significant
Koch et al.[22]	0.285 ± 0.05	0.36 ± 0.08	Significant
Baleanu et al.[35]	0.30 ± 0.1	0.34 ± 0.08	Not significant
Salvetti et al.[55]	0.23 ± 0.13	0.29 ± 0.18	Significant
Rizzoni et al.[54]	0.264 ± 0.11	0.37 ± 0.09	Significant

All cited studies find the same trend but use different measurement technologies and somewhat different populations. Significances are based on stated results from studies.

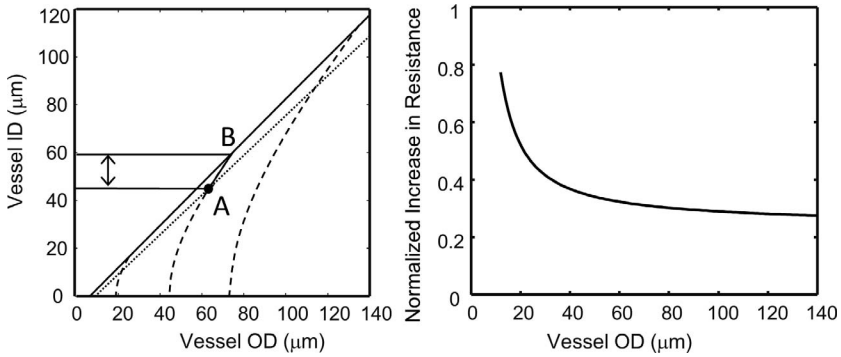

Figure 7. Evaluating the impact of eutrophic remodeling on vascular measurements. *Left*: The *solid line* shows the measured relation between ID and OD for LTN subjects ($r^2 = 0.99$). *Dashed curves* show how individual vessels would be affected with increased eutrophic remodeling. Thus, if we measure a vessel with OD and ID as represented by point A, it would presumably, prior to hypertensive remodeling, have been located at point B. This implies that the vessel changed its inner diameter as shown by the *double headed arrow*. *Right*. The computed normalized change in resistance based on a fourth power relation between lumen size and resistance. Note that the largest resistance changes occurred for our measured small vessels, however their total length is relatively small, which supports the idea that the largest changes in total systemic resistance do not arise from the smallest vessels.

difference was within the 95% confidence limits and so we were unable to reject hypertrophic remodeling.

Our second question was how remodeling would impact vascular resistance. Although the systemic resistance vessels are generally considered to be small arteries in the range of 100 to 450 μm OD,[57] our results suggest that the largest WLR changes are in the smallest arterioles (Fig. 4). To evaluate the impact on vascular resistance we assumed that WCSA was conserved as in Figure 7. We then calculated from the curves the "initial" ID of the hypertensives' arterioles from the measured ID and OD of the vessel and assumed that vascular resistance is proportional to the inverse fourth power of the lumen radius (Pouseille's law), and no other parameters (viscosity, etc.) change. We then calculated the difference between the resistance given by the measured ID and the calculated "initial" resistance and then divided by the "initial" resistance. As expected the resistance increases with remodeling (Fig. 7, right) and the increase is largest for the smallest vessels. However, because the distance traveled within a small vessel is short, approximately 150 μm,[33] it is unlikely that these vessels are a major determinant of the increased systemic vascular resistance in HTN. The curve tapers to an increase in resistance of about 30% for larger arterioles and because of the distribution of vessel lengths within the eye, it is this asymptotic value that is likely to represent the overall change in resistance within the eye. While there are other possible forms of remodeling, given that our subject hypertensive population consisted of managed essential hypertensive patients, eutrophic remodeling is the most likely mechanism for an increase in vascular resistance. We also performed this calculation based on a simple direct comparison of vessels (assuming the OD remained the same and only the ID changed, and this produced a similar conclusion).

It is unknown whether the simple linear relation between ID and OD that we measure for the eye represents a property of the systemic circulation or is organ specific. If this is generalizable, it opens the possibility of evaluating a patient's current vascular wall structure compared with this basal state. This would provide an estimate of a given patient's vascular status arising from hypertension or diabetes. This would aid in 'individualized' medicine by allowing estimation of the effects disease in a new patient and thus delivery of more appropriate care than depending on surrogate measures of vascular health such as blood pressure. Although its medical use is dependent on the establishment of correlations between ocular vascular change and systemic vascular consequences such as renal or cardiac damage and possibly even Alzheimer's disease; it is reasonable that precise measurements over a greater range of vascular sizes could yield improved clinical patient stratification and prognostication. To test this concept on the current data set we used the linear fits to the LTN data of Figure 2. We computed the difference between the predicted and actual ID of each measurement of OD and averaged these for each subject. The group results are shown in Figure 8. The LTN subjects fall close to the prediction as expected. The NTN subjects overlap the LTN data but there are numerous outliers with smaller ID. Every individual in our HTN group

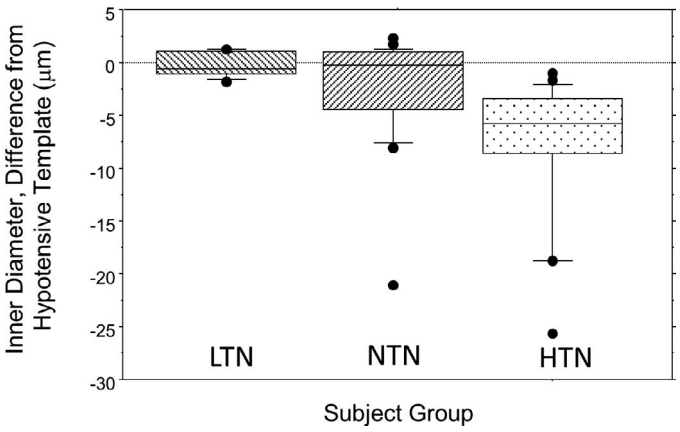

Figure 8. Box plots of the residual for each subject group compared with the template curve achieved by fitting the LTN data of Figure 2 with a linear model ($r^2 > 0.99$). Actual measurements for each vessel in each subject were then subtracted from the predicted value for that size vessel, and then the average residual computed for each subject and the averages for groups plotted. The LTN group is close to the template (as expected) and the range of residuals is very small. For the NTN and HTN groups the data diverge from the template. Box plots as in Figure 5.

fell outside the 95% confidence limits for the LTN subject. While a larger scale, well-controlled clinical study is desirable, the current results are encouraging.

The main limitations of the current study include the relatively small sample size and the lack of control for lifestyle factors, age, or sex. A consensus has not been reached on how age or gender affect WLR[22,44,55] and subdividing our subject population results in numbers too small to be meaningful statistically and in fact our low-tension group was primarily female (Table 1). Other limitations are that our hypertensive subject group was not stratified by medication or degree or duration of blood pressure elevation and also some members of the NTN group could have been prehypertensive. Because these factors were not controlled for, the overall diversity within each pressure group may have increased the within group variability, created a bias, or both. However, the increased variability should have decreased statistical power, yet we found the differences were highly significant and so we do not believe this limitation weakens our results, but rather that better classification of a larger study should most likely increase the effect that was seen and help resolve age, sex, and racial differences in vascular wall structure.

In conclusion, the use of multiply scattered light AOSLO retinal imaging allowed us to extend the range of vessel sizes for which in vivo vascular structure could be accurately measured. Results suggest that the largest relative changes in resistance to blood flow in HTN could occur at the smallest sizes of arterioles, certainly within the eye and possibly elsewhere in the body. This level of vasculature is distinctly smaller than the usual class of arterioles considered as the primary resistance vessels, and our results do not contradict the general consensus, because while the change per vessel is large, the effective length is small. The very high correlation of the ID and OD for the arterioles in LTN subjects is suggestive that, at least in the eye, a proportional relation may exist between ID and OD, which is then modified through eutrophic or hypertrophic remodeling in individuals with higher blood pressures. This data may allow more accurate studies of hypertensive vascular remodeling and of clinically observable vascular alterations seen in other diseases such as diabetes, by allowing patients to be compared with a basal vascular wall template. Further research is clearly required to validate these concepts.

Acknowledgments

Portions of this work were presented at the Association for Research in Vision and Ophthalmology annual meeting (Hillard, Chui, Gast, Sapir, Burns Adaptive Optics Measurements of Retinal Arterial Wall Thickness in both Normotensive and Hypertensive Subjects, ARVO, 2013).

Supported by grants from the National Institutes of Health Grants EY024315 and P30EY019008 and Foundation Fighting Blindness Grant TA-CL-0613-0617-IND and a Fight for Sight summer research grant.

Disclosure: **J.G. Hillard,** None; **T.J. Gast,** None; **T.Y.P. Chui,** None; **D. Sapir,** None; **S.A. Burns,** AEON Imaging

References

1. Cheung N, Wong TY. Diabetic retinopathy and systemic vascular complications. *Prog Ret Eye Res*. 2008;27:161–176.
2. Ikram MK, Cheung CY, Lorenzi M, et al. Retinal vascular caliber as a biomarker for

diabetes microvascular complications. *Diabetes Care*. 2013;36:750–759.
3. Schmieder RE. Hypertensive retinopathy - a window to vascular remodeling in arterial hypertension. *Hypertension*. 2008;51:43–44.
4. Ritt M, Harazny JM, Ott C, et al. Impaired increase of retinal capillary blood flow to flicker light exposure in arterial hypertension. *Hypertension*. 2012;60:871–876.
5. Wong T, Mitchell P. The eye in hypertension. *Lancet*. 2007;369:425–435.
6. Cheung N, Wang JJ, Klein R, Couper DJ, Sharrett AR, Wong TY. Diabetic retinopathy and the risk of coronary heart disease - The Atherosclerosis Risk in Communities Study. *Diabetes Care*. 2007;30:1742–1746.
7. Klein R, Klein BEK, Moss SE, Wong TY. Retinal vessel caliber and microvascular and macrovascular disease in type 2 diabetes - XXI: The Wisconsin Epidemiologic Study of Diabetic Retinopathy. *Ophthalmology*. 2007;114:1884–1892.
8. Wolf S, Arend O, Tonnen H, Bertram B, Jung F, Reim M. Retinal capillary blood flow measurements by means of scanning laser ophthalmoscope preliminary results. *Ophthalmology*. 1991;98:996–1000.
9. Webb RH, Hughes GW, Delori FC. Confocal scanning laser ophthalmoscope. *Applied Opt*. 1987;26:1492–1499.
10. Ikram MK, Witteman JCM, Vingerling JR, Breteler MMB, Hofman A, de Jong P. Retinal vessel diameters and risk of hypertension - The Rotterdam Study. *Hypertension*. 2006;47:189–194.
11. Lim M, Sasongko MB, Ikram MK, et al. Systemic associations of dynamic retinal vessel analysis: a review of current literature. *Microcirculation*. 2013;20:257–268.
12. Liang J, Williams DR, Miller DT. Supernormal vision and high-resolution retinal imaging through adaptive optics. *J Opt Soc Am A*. 1997;14:2884–2892.
13. Burns SA, Marcos S, Elsner AE, Bara S. Contrast improvement of confocal retinal imaging by use of phase-correcting plates. *Opt Lett*. 2002;27:400–402.
14. Roorda A, Romero-Borja F, Donnelly WJ, Hebert TJ, Queener H. Dynamic imaging of microscopic retinal features with the adaptive optics scanning laser ophthalmoscope. *Invest Ophthalmol Vis Sci*. 2002;43:U1261–U1261.
15. Wang Q, Kocaoglu OP, Cense B, et al. Imaging retinal capillaries using ultrahigh-resolution optical coherence tomography and adaptive optics. *Invest Ophthalmol Vis Sci*. 2011;52:6292–6299.
16. Tam J, Dhamdhere KP, Tiruveedhula P, et al. Subclinical capillary changes in non-proliferative diabetic retinopathy. *Optom Vis Sci*. 2012;89:E692–E703.
17. Bedggood P, Metha A. Direct visualization and characterization of erythrocyte flow in human retinal capillaries. *Biomed Opt Express*. 2012;3:3264–3277.
18. Tsujikawa A, Ogura Y. Evaluation of leukocyte-endothelial interactions in retinal diseases. *Ophthalmologica*. 2012;227:68–79.
19. Deak GG, Schmidt-Erfurth U. Imaging of the parafoveal capillary network in diabetes. *Current Diabetes Reports*. 2013;13:469–475.
20. Lombardo M, Parravano M, Serrao S, Ducoli P, Stirpe M, Lombardo G. Analysis of retinal capillaries in patients with type 1 diabetes and nonproliferative diabetic retinopathy using adaptive optics imaging. *Retina*. 2013;33:1630–1639.
21. Bedggood P, Metha A. Analysis of contrast and motion signals generated by human blood constituents in capillary flow. *Opt Lett*. 2014;39:610–613.
22. Koch E, Rosenbaum D, Brolly A, et al. Morphometric analysis of small arteries in the human retina using adaptive optics imaging: relationship with blood pressure and focal vascular changes. *J Hypertens*. 2014;32:890–898.
23. Huang D, Swanson EA, Lin CP, et al. Optical coherence tomography for micron-resolution imaging. *Science*. 1991;254:1178–1181.
24. Izatt JA, Hee MR, Huang D, et al. Micron-resolution biomedical imaging with optical coherence tomography. *Opt Photon News*. 1993;4:14–19.
25. Chui TYP, Zhong ZY, Song HX, Burns SA. Foveal avascular zone and its relationship to foveal pit shape. *Optom Vis Sci*. 2012;89:602–610.
26. Chui TYP, VanNasdale DA, Burns SA. The use of forward scatter to improve retinal vascular imaging with an adaptive optics scanning laser ophthalmoscope. *Biomed Opt Express*. 2012;3:2537–2549.
27. Chui TY, Gast TJ, Burns SA. Imaging of vascular wall fine structure in the human retina using adaptive optics scanning laser ophthalmoscopy. *Invest Ophthalmol Vis Sci*. 2013;54:7115–7124.
28. Pinhas A, Dubow M, Shah N, et al. In vivo imaging of human retinal microvasculature using adaptive optics scanning light ophthalmoscope

fluorescein angiography. *Biomed Opt Express*. 2013;4:1305–1317.
29. Burns SA, Elsner AE, Chui TY, et al. In vivo adaptive optics microvascular imaging in diabetic patients without clinically severe diabetic retinopathy. *Biomed Opt Express*. 2014;5:961–974.
30. Sulai YN, Scoles D, Harvey Z, Dubra A. Visualization of retinal vascular structure and perfusion with a nonconfocal adaptive optics scanning light ophthalmoscope. *J Opt Soc Am A*. 2014;31:569–579.
31. Rizzoni D, Agabiti-Rosei E. Structural abnormalities of small resistance arteries in essential hypertension. *Internal and Emergency Medicine*. 2012;7:205–212.
32. Castorena-Gonzalez JA, Staiculescu MC, Foote C, Martinez-Lemus LA. Mechanisms of the inward remodeling process in resistance vessels: is the actin cytoskeleton involved? *Microcirculation*. 2014;21:219–229.
33. Caro CG, Pedley TJ, Schroter RC, Seed WA. *The Mechanics of the Circulation*. City: Cambridge University Press; 2011.
34. Feihl F, Liaudet L, Waeber B. The macrocirculation and microcirculation of hypertension. *Curr Hypertens Rep*. 2009;11:182–189.
35. Baleanu D, Ritt M, Harazny J, Heckmann J, Schmieder RE, Michelson G. Wall-to-lumen ratio of retinal arterioles and arteriole-to-venule ratio of retinal vessels in patients with cerebrovascular damage. *Invest Ophthalmol Vis Sci*. 2009;50:4351–4359.
36. Intengan HD, Schiffrin EL. Vascular remodeling in hypertension: roles of apoptosis, inflammation, and fibrosis. *Hypertension*. 2001;38:581–587.
37. Buus NH, Mathiassen ON, Fenger-Gron M, et al. Small artery structure during antihypertensive therapy is an independent predictor of cardiovascular events in essential hypertension. *J Hypertens*. 2013;31:791–797.
38. Ritt M, Harazny JM, Ott C, et al. Analysis of retinal arteriolar structure in never-treated patients with essential hypertension. *J Hypertens*. 2008;26:1427–1434.
39. Heagerty AM, Heerkens EH, Izzard AS. Small artery structure and function in hypertension. *J Cell Mol Med*. 2010;14:1037–1043.
40. Rizzoni D, De Ciuceis C, Porteri E, et al. Altered structure of small cerebral arteries in patients with essential hypertension. *J Hypertens*. 2009;27:838–845.
41. Heerkens EHJ, Izzard AS, Heagerty AM. Integrins, vascular remodeling, and hypertension. *Hypertension* 2007;49:1–4.
42. Aalkjaer C, Heagerty AM, Bailey I, Mulvany MJ, Swales JD. Studies of isolated resistance vessels from offspring of essential hypertensive patients. *Hypertension*. 1987;9:155–158.
43. Lehmann MV, Schmieder RE. Remodeling of retinal small arteries in hypertension. *Am J Hypertens*. 2011;24:1267–1273.
44. Harazny JM, Ritt M, Baleanu D, et al. Increased wall: Lumen ratio of retinal arterioles in male patients with a history of a cerebrovascular event. *Hypertension*. 2007;50:623–629.
45. Elsner AE, Miura M, Stewart JB, Kairala MBM, Burns SA. Novel algorithms for polarization imaging resulting in improved quantification of retinal blood vessels. In: Westwood JD, Hoffman HM, Mogel GT, Phillips R, Robb RA, Stredney D, eds. *Medicine Meets Virtual Reality 11: Nextmed: Health Horizon*. Washington, DC: IOS Press; 2003:59–61.
46. Ferguson RD, Zhong Z, Hammer DX, et al. Adaptive optics scanning laser ophthalmoscope with integrated wide-field retinal imaging and tracking. *J Opt Soc Am A*. 2010;27:A265–A277.
47. Zou WY, Qi XF, Burns SA. Woofer-tweeter adaptive optics scanning laser ophthalmoscopic imaging based on Lagrange-multiplier damped least-squares algorithm. *Biomed Opt Express*. 2011;2:1986–2004.
48. Zou WY, Qi XF, Huang G, Burns SA. Improving wavefront boundary condition for in vivo high resolution adaptive optics ophthalmic imaging. *Biomed Opt Express*. 2011;2:3309–3320.
49. Huang G, Qi X, Chui TY, Zhong Z, Burns SA. A clinical planning module for adaptive optics SLO imaging. *Optom Vis Sci*. 2012;89:593–601.
50. Burns SA, Tumbar R, Elsner AE, Ferguson D, Hammer DX. Large-field-of-view, modular, stabilized, adaptive-optics-based scanning laser ophthalmoscope. *J Opt Soc Am A*. 2007;24:1313–1326.
51. Group Authors: ANSI, American National Standards for safe use of lasers, ANSI Z136, 2014, Orlando, FL.
52. Huang G, Zhong ZY, Zou WY, Burns SA. Lucky averaging: quality improvement of adaptive optics scanning laser ophthalmoscope images. *Opt Lett*. 2011;36:3786–3788.
53. Bennett AG, Rudnicka AR, Edgar DF. Improvements on littmann method of determining the size of retinal features by fundus photography. *Graefes Arch Clin Exp Ophthalmol*. 1994;232:361–367.
54. Rizzoni D, Porteri E, Duse S, et al. Relationship between media-to-lumen ratio of subcutaneous small arteries and wall-to-lumen ratio of retinal arterioles evaluated noninvasively by scanning

laser Doppler flowmetry. *J Hypertens*. 2012;30: 1169–1175.
55. Salvetti M, Rosei CA, Paini A, et al. Relationship of wall-to-lumen ratio of retinal arterioles with clinic and 24-hour blood pressure. *Hypertension*. 2014;63:1110–1115.
56. Mulvany MJ. Small artery remodeling in hypertension. *Curr Hypertens Rep*. 2002;4:49–57.
57. Mulvany MJ, Aalkjaer C. Structure and function of small arteries. *Physiological Rev*. 1990;70:921–961.